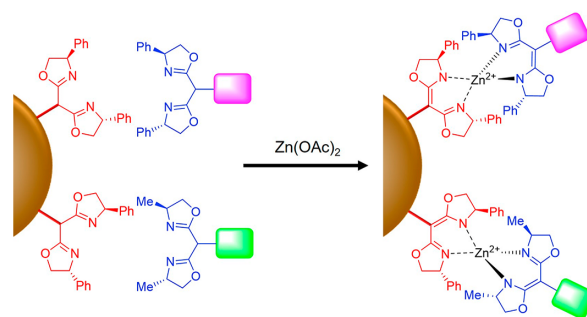


Multi-Functionalization of Solid Support via Zn(II)-Mediated Chirality-Directed Self-Assembly

Max S. Overshiner^aShuyuan Tian^aKegan B. Morrow^aJailyn R. Wendt^aJohn Zhou^aHannah M. Briggs^aGerardo B. Márquez^aKathleen V. Kilway^aShin A. Moteki^{* a}

^a Division of Energy, Matter, and System, School of Science and Engineering, University of Missouri – Kansas City, Kansas City, Missouri 64110, USA

* motekis@umkc.edu



Quantitative Multi-Functionalization via Chirality-Driven Self-Assembly

Received: 18.02.2023

Accepted after revision: 30.05.2023

DOI: 10.1055/a-2106-9071; Art ID: OM-2023-02-0002-OA

License terms:

© 2023. The Author(s). This is an open access article published by Thieme under the terms of the Creative Commons Attribution License, permitting unrestricted use, distribution, and reproduction so long as the original work is properly cited. (<https://creativecommons.org/licenses/by/4.0/>).

Abstract Establishing a strategy for realizing programmed self-assembly is critical in manufacturing materials with functional hybrid structures. In this work, we introduce a robust methodology for enabling multi-component self-assembly using the concept of chirality-directed self-assembly. A specific combination of heterochiral Zn(II) methylene bis(oxazoline) (BOX) complexes can be selectively generated when combinations of enantiomers of chiral BOX ligands are mixed in the presence of Zn(OAc)₂. The resulting Zn(II) BOX complexes, unlike non-covalent bonds, are highly stable and stay intact at elevated temperatures, yet can be reversibly disintegrated under mild conditions using EDTA. This approach can be easily applied to multi-functionalize various solid supports enabling the one-pot generation of multi-functional hybrid structures.

Key words: chirality-driven self-assembly, multi-functionalization, heterochiral metal–ligand complexes

Introduction

Multi-component self-assembly is critical in the construction of functional hybrid structures from various building blocks, constructing structurally complex and functional architectures for various applications.¹ The process of self-assembly,² where building units of a system are organized into an ordered and/or functional structure, has attracted researchers from a diverse range of disciplines that vary from chemistry and materials science to engineering and technology.³

The assembly through covalent bonds⁴ has the advantage of being independent of and unaffected by solvent conditions, such as solvent polarity and ionic strength.⁵ However, the generation of covalent bonds often raises challenges due to the compatibility of reagents and reaction conditions for functional groups within building units.⁶ This issue often results in significant limitations in the diversity of assembling functional groups. In contrast, using non-covalent bonds⁷ reduces the risk of their reaction compatibility due to their mild assembly conditions. In addition, highly reversible bonds allow multi-functional structures disassemble back into individual building units, enabling the recycling of these small units.⁸ Unfortunately, their inherent weaker bond strengths, which are highly sensitive to environmental conditions such as solvent polarity, temperature, ionic strength, and pH, often severely limit their range of applications.⁹ To this end, reversible metal–ligand complexes¹⁰ have higher stability under a broader range of reaction conditions/environments and can be assembled in situ under mild conditions. Most examples utilize combinations of metal and achiral ligands for self-assembly, and a lack of selectivities among achiral ligands often leads to challenges in controlling the overall shapes and sizes of supramolecules. To this end, we recently reported a versatile approach to preparing resin-immobilized catalysts through metal–ligand complexes.¹¹ Our unique approach utilizes the concept of chirality-directed self-assembly¹² where chiral bis(oxazoline) (BOX) ligands with complementary chirality selectively form a heterochiral Zn(II) complex,¹³ anchoring a catalyst onto the resin. In other words, when equimolar amounts of chiral BOX ligands with opposite enantiomers were mixed in the presence of Zn(OAc)₂, exclusive formation of the heterochiral Zn(II) complex was observed. The high selectivity toward the formation of the heterochiral Zn(II) BOX complex arises from reduced steric crowding of the

phenyl rings on the chiral BOX ligand around the Zn(II) center.¹⁴ The Zn(II) center on the homochiral Zn(II) complex is destabilized by adopting a distorted tetrahedral geometry to accommodate two phenyl substituents in the same quadrant (Figure 1). The loaded catalyst can be altered in situ through ligand exchange for 2-step sequential reactions using the same resin. The report demonstrated that resin-bound catalysts could be easily recycled under mild conditions without damaging resin functional groups, helping to reduce the generation of microparticle wastes.

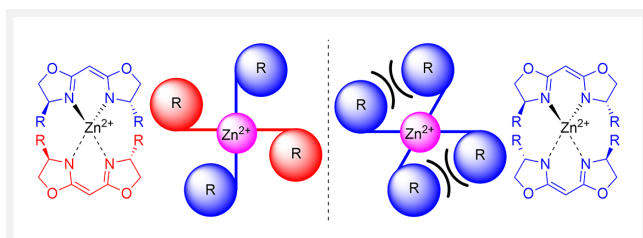
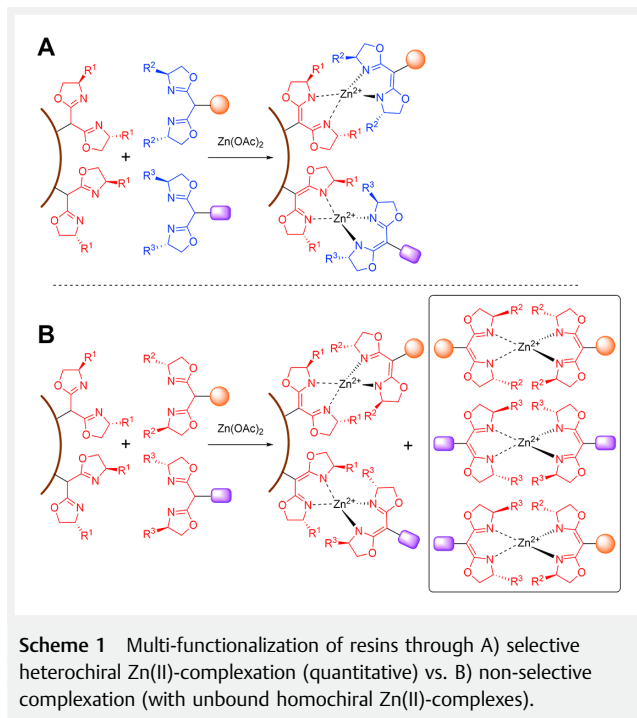


Figure 1 The difference in stability between heterochiral Zn(II) complex (left) vs. homochiral Zn(II) complex (right).

The concept of chirality-directed self-assembly was also employed to quantitatively generate distinct Janus dendrimers in situ from various dendron subunits attached to chiral BOX ligands.¹⁵ The highly selective formation of the heterochiral Zn(II) complex at the focal point of the Janus dendrimer enables the exclusive formation of Janus dendrimer upon mixing two distinct dendritic domains, each functionalized by opposite enantiomer of BOX ligands. The heterochiral Zn(II) BOX complex at the focal point was stable under elevated temperature. However, the complex can be reversibly disintegrated under mild conditions with the use of EDTA.

These previous studies have led us to believe that resin multi-functionalization is possible if we identify sets of chiral BOX ligands that selectively form multiple Zn(II) BOX complexes on the resin surface.^{1,5,16} In other words, to realize the multi-functionalization of the solid support, the interaction between the BOX ligand immobilized on the solid support and added ligands must be highly selective (Scheme 1A). Lack of such selectivity led to a non-selective complexation, resulting in the generation of wasteful unbound catalysts (Scheme 1B); therefore, difficult to control the relative ratio of the functional groups on the resin. Hence, our goal here is to identify the optimum sets of chiral BOX ligands generating highly selective Zn(II) BOX complexes to establish a versatile one-pot approach for the multi-functionalization of solid support.

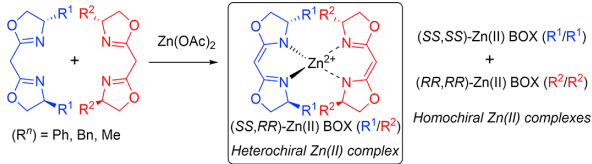


Scheme 1 Multi-functionalization of resins through A) selective heterochiral Zn(II)-complexation (quantitative) vs. B) non-selective complexation (with unbound homochiral Zn(II)-complexes).

Results and Discussion

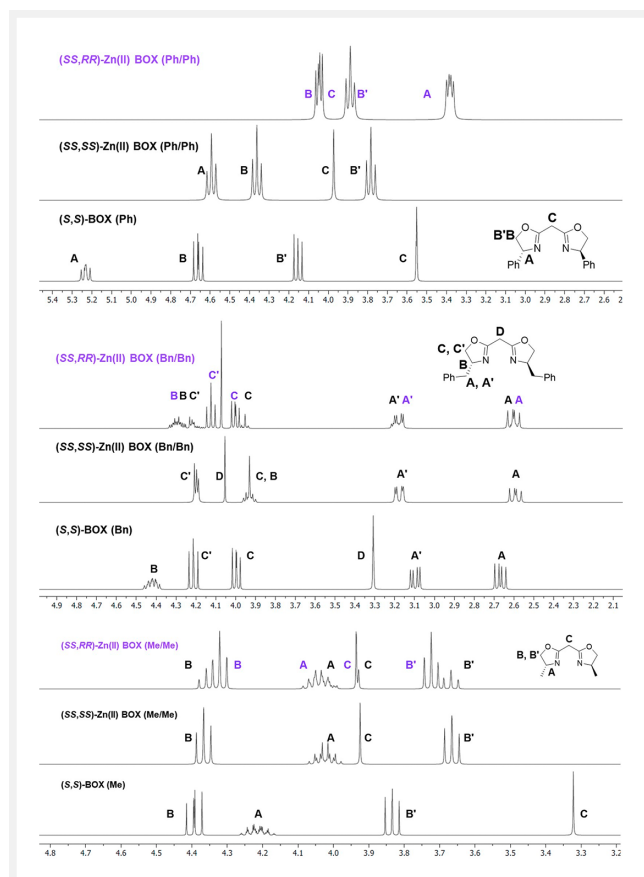
Comprehensive studies on the relative stability of various homo- and heterochiral Zn(II) BOX complexes have not been reported thus far (Scheme 1A vs. 1B). Therefore, we decided to elucidate the efficiency in generating heterochiral Zn(II) complexes to identify the correlation between the size of chiral substituents and selectivity toward forming heterochiral Zn(II) complexes (Table 1). For this investigation, the ratio of heterochiral vs. homochiral Zn(II) BOX complexes was measured using ¹H NMR spectroscopy in CDCl₃ (Figure 2).

The exclusive formation of the heterochiral Zn(II) complex (*SS,RR*)-Zn(II) BOX (Ph/Ph) was observed when equimolar amounts of (*S,S*)-BOX (Ph) and (*R,R*)-BOX (Ph) were used (Table 1, entry 1; Figure 2, top). The ligand exchange process was instantaneous, and no homochiral Zn(II) complexes nor free ligands remained in the solutions. By contrast, when the steric bulkiness was moved further away from the chiral center on the oxazoline ring, as steric interactions among chiral substituents in the homochiral Zn(II) complex is reduced, selectivity toward the heterochiral Zn(II) complex was reduced. For instance, the benzyl-substituted chiral BOX's Zn(II) complex reached equilibrium at ambient temperature with 25% homochiral Zn(II) complexes remaining in the solution (Table 1, entry 2; Figure 2, middle).¹⁷ Interestingly, similar selectivity was obtained with methyl-substituted chiral BOX (Table 1, entry 3; Figure 2, bottom).

Table 1 The efficiency of the generation of the heterochiral Zn(II) BOX complexes using (*S,S*)- and (*R,R*)-BOX ligands with various substituents


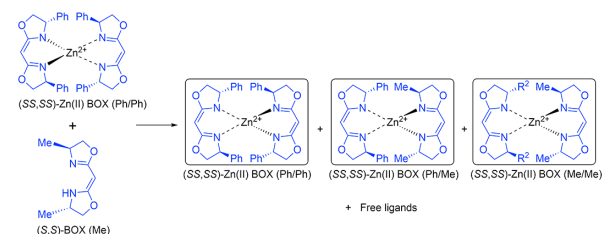
Entry	(R1/R2) ^a	Heterochiral Zn(II) complex (%)	Homochiral Zn(II) complexes (%)
1	Ph/Ph	>99	0
2 ^b	Bn/Bn	77	23
3 ^b	Me/Me	72	28
4 ^b	Me/Bn	73	27

^a Chirality color code: R1 = substituent on the (*S,S*)-BOX and R2 = substituent on the (*R,R*)-BOX; ^b % ratio was calculated after 0.5 h of incubation at ambient temperature. The ratio remained the same after 5 days at ambient temperature.

**Figure 2** ¹H NMR spectrum of the free ligand, homochiral Zn(II) complex, and heterochiral Zn(II) complex of chiral BOX ligands (top: Ph-substituted, middle: Bn-substituted, and bottom: Me-substituted).

In addition, when equimolar amounts of (*RR,RR*)-Zn(II) BOX (Bn) and (*SS,SS*)-Zn(II) BOX (Me) were mixed, the outcome of selectivity toward generating the heterochiral Zn(II) complex ((*SS,RR*)-Zn(II) BOX (Me/Bn)) was identical to the cases with (*SS,RR*)-Zn(II) BOX (Me) and (*SS,RR*)-Zn(II) BOX (Bn) (entry 4).¹⁸ These results indicate that steric effect at the C1 position on the chiral substituent is significant in the outcome of chiral discrimination processes.

Next, to probe stability differences among homochiral Zn(II) complexes (Scheme 1B), a free ligand titration experiment was conducted as shown in Table 2. When 1 equiv of free (*S,S*)-BOX (Me) ligand was added to the homochiral (*SS,SS*)-Zn(II) BOX (Ph), a mixture of three homochiral zinc complexes, (*SS,SS*)-Zn(II) BOX (Ph), (*SS,SS*)-Zn(II) BOX (Ph/Me), and (*SS,SS*)-Zn(II) BOX (Me), was formed in a ratio 1.0:2.0:1.4 in favor of (*SS,SS*)-Zn(II) BOX (Ph/Me) through a rapid ligand exchange (entry 1 vs. 2).

Table 2 Ligand exchange experiments adding a free BOX ligand (*S,S*)-BOX (Me) to the homochiral complex (*SS,SS*)-Zn(II)-(Ph/Ph)


Entry	(<i>S,S</i>)-BOX (Me) (equiv)	(<i>SS,SS</i>)-Zn(II) BOX % distribution ^a		
		(<i>SS,SS</i>)-Zn(II) BOX (Ph/Ph) (%)	(<i>SS,SS</i>)-Zn(II) BOX (Ph/Me) (%)	(<i>SS,SS</i>)-Zn(II) BOX (Me/Me) (%)
1	0	>99	0	0
2	1.0	23	45	32
3	2.0	0	32	68
4	4.0	0	0	>99

^a Calculated based on ¹H NMR integration of the homochiral Zn(II) complexes without including free ligands.

Further addition of free (*S,S*)-BOX (Me) led to the complete disappearance of (*SS,SS*)-Zn(II) BOX (Ph/Ph), leaving two homochiral (*SS,SS*)-Zn(II) BOX (Ph/Me) and (*SS,SS*)-Zn(II) BOX (Me) in solution with a ratio of 1:2:1 (entry 3). The complete conversion to (*SS,SS*)-Zn(II) BOX (Me/Me) was reached when 4 equiv of free (*S,S*)-BOX (Me) was added to (*SS,SS*)-Zn(II) BOX (Ph) (entry 4).

To achieve the quantitative multi-functionalization of the solid support (Scheme 1A), combinations of chiral ligands must be carefully chosen to avoid generating wasteful unbound complexes. To this end, based on the results above, the heterochiral Zn(II) complexes showed higher stabilities than all of the homochiral Zn(II) complexes studied here. In-

deed, the heterochiral (SS,RR) -Zn(II) BOX (Me/Ph) formed quantitatively when opposite enantiomers of (RR,RR) -Zn(II) BOX (Ph/Ph) and (SS,SS) -Zn(II) BOX (Me/Me) were mixed, leaving no homochiral Zn(II) complexes remaining in the solution (Figure 3-1).¹⁹

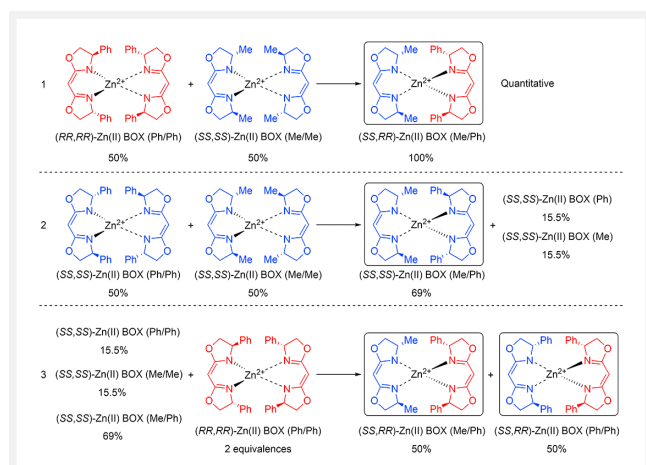


Figure 3 Generation of two specific heterochiral Zn(II) BOX complexes from three homochiral Zn(II) complexes.

In contrast, using a pair of homochiral Zn(II) complexes, (SS,SS) -Zn(II) BOX (Ph/Ph) and (SS,SS) -Zn(II) BOX (Me/Me), similar experiments afforded a mixture of homochiral Zn(II) complexes in solution (Figure 3-2). Combined results from above, this result strongly indicates the higher stability of heterochiral Zn(II) complexes over any combination of homochiral Zn(II) complexes. To this end, when 2 equiv of (RR,RR) -Zn(II) BOX (Ph/Ph) was added to this mixture of homochiral Zn(II) complexes, and all complexes were converted to a combination of heterochiral Zn(II) complexes ((SS,RR) -Zn(II) BOX (Me/Ph) and (SS,RR) -Zn(II) BOX (Ph/Ph)) (Figure 3-3, Figure 4, top). In other words, the selective generation of heterochiral Zn(II) complexes can be accom-

plished by mixing (RR,RR) -Zn(II) BOX (Ph/Ph), (SS,SS) -Zn(II) BOX (Ph/Ph), and (SS,SS) -Zn(II) BOX (Me/Me) in a 2 : 1 : 1 ratio resulting in the selective formation of (SS,RR) -Zn(II) BOX (Me/Ph) and (SS,RR) -Zn(II) BOX (Ph/Ph) in situ. Identical results were obtained through mixing combinations of free ligands (R,R) -Zn(II) BOX (Ph), (S,S) -Zn(II) BOX (Ph), and (S,S) -Zn(II) BOX (Me) in a 2 : 1 : 1 ratio along with $Zn(OAc)_2$. When the ratio of (SS,SS) -Zn(II) BOX (Ph) and (SS,SS) -Zn(II) BOX (Me) was altered (2 : 1), the final ratio of (SS,RR) -Zn(II) BOX (Me/Ph) and (SS,RR) -Zn(II) BOX (Ph/Ph) was also altered, identical to the initial mixture ratio of two homochiral Zn(II) complexes. Within a temperature range tested (25 – 125 °C in DMSO-*d*⁶), no differences in thermal stability between (SS,RR) -Zn(II) BOX (Me/Ph) and (SS,RR) -Zn(II) BOX (Ph/Ph) were observed. In other words, both complexes were intact at elevated temperatures, and no disintegration of complexes was observed. These experiments suggest that chirality-driven self-assembly can load multiple functional groups quantitatively through metal–ligand complexes onto the resin without generating wasteful unbound ligands.

To probe the applicability of the chirality-driven self-assembly for the multi-functionalization of resin depicted in Scheme 1A, we decided to use (R,R) -BOX-immobilized Wang resin,²⁰ which we have previously used to demonstrate a single functionalization of resin through self-assembly. As previously demonstrated, the functional loading capacity of the (R,R) -BOX-immobilized Wang resin was calculated by the standard Fmoc-quantification approach and determined to be 0.28 mmol/g.²¹ The generation of heterochiral Zn(II) BOX on the resin was achieved by mixing (R,R) -BOX-immobilized Wang resin with free (S,S) -BOX ligands in the presence of an equimolar amount of $Zn(OAc)_2$. The formation of heterochiral Zn(II) complexes on the resin was monitored through FTIR analysis. Any unbound free ligand and free Zn(II) complexes can be detected by ¹H NMR spectroscopy by analyzing the supernatant solution.

When the equimolar BOX ligand, (S,S) -BOX (Ph), was added to the (R,R) -BOX (Ph)-functionalized Wang resin along with $Zn(OAc)_2$, no free ligands or unbound homochiral Zn(II) BOX (Ph) complexes were detected in the supernatant solution ($CDCl_3$) (Table 3, entry 1). FTIR analysis shows that the C=N stretch shifted from 1655 cm^{-1} (uncomplexed (R,R) -BOX (Ph) on a resin) to 1601 cm^{-1} (complexed) (Figure 5A vs. 5B), and the results are consistent with previously observed values.^{22,23} The functionalization of resin required $Zn(OAc)_2$ as its absence results in quantitative recovery of (S,S) -BOX (Ph) from the supernatant solution (entry 2). The resin-bound heterochiral Zn(II) complex, (SS,RR) -Zn(II) BOX (Ph/Ph), remained intact and the complex did not disintegrate when the resin was heated up to 160 °C for 72 h in *d*₆-DMSO. However, the treatment with EDTA disintegrated the complex, and then the released (S,S) -BOX (Ph) was recovered quantitatively from the supernatant solution.

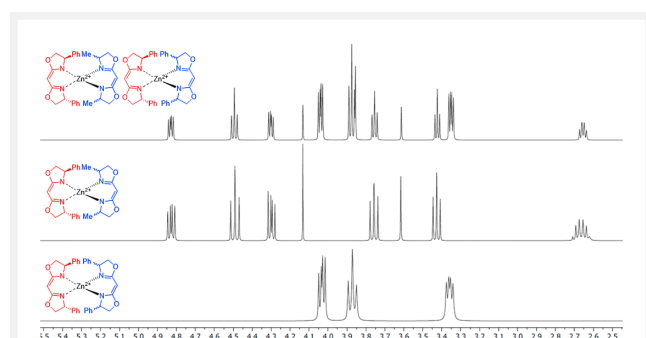
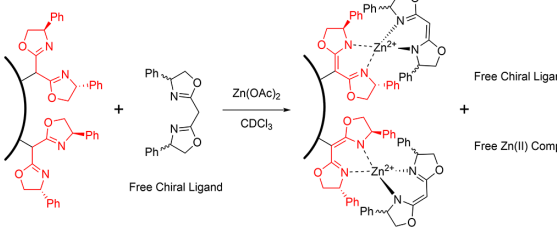


Figure 4 Comparison of ¹H NMR spectra: (SS,RR) -Zn(II) BOX (Ph/Ph) (bottom), (SS,RR) -Zn(II) BOX (Me/Ph) (middle), and formation of two specific heterochiral Zn(II) BOX complexes (top).

Table 3 A single functionalization of Wang resin through chirality-directed self-assembly


Entry	Added free ligand ^a	Product	
		Bound	Unbound
1	(<i>S,S</i>)-BOX (Ph)	>98%	ND ^d
2	(<i>S,S</i>)-BOX (Ph) ^b	ND ^d	>98%
3 ^c	(<i>R,R</i>)-BOX (Ph)	46%	54%

^a Equimolar amounts (0.28 mmol/g) of ligand and Zn(OAc)₂ were added to the suspended resin; ^b (*S,S*)-BOX (Ph) was mixed with suspended resin in the absence of Zn(OAc)₂; ^c No free ligand was observed in the supernatant solution.; ^d ND: not detected.

The FTIR analysis of EDTA-treated resin shows the C=N stretch at 1655 cm⁻¹, indicating that the (*R,R*)-BOX (Ph) covalently attached to the resin was not affected by the EDTA treatment. In fact, the heterochiral Zn(II) BOX can be regenerated on the EDTA-treated resin by mixing an equimolar amount of (*S,S*)-BOX (Ph) along with Zn(OAc)₂. In sharp contrast to the formation of the heterochiral Zn(II) complex on the resin, the efficiency in forming homochiral Zn(II) complex, using (*R,R*)-BOX (Ph), on the resin was not efficient as almost half of the added ligand formed unbound homochiral Zn(II) complex in solution (entry 3). These results support that using chiral BOX ligands with complementary chirality led to quantitative loading of the functional group on the resin.

Encouraged by the results above, a quantitative formation of two distinct heterochiral Zn(II) complexes on the (*R,R*)-BOX (Ph)-functionalized Wang resin was investigated. When 0.5 equiv of each (*S,S*)-BOX (Ph) and (*S,S*)-BOX (Me) were mixed with the (*R,R*)-BOX (Ph)-functionalized resin in the presence of Zn(OAc)₂, these added free ligands quickly disappeared from the supernatant solution (Table 4, entry 1). The FTIR analysis of the resin indicated a generation of two heterochiral Zn(II) complexes on a resin with two C=N stretches, 1598 cm⁻¹ ((*SS,RR*)-Zn(II) BOX (Ph/Ph)) and 1593 cm⁻¹ ((*SS,RR*)-Zn(II) BOX (Me/Ph)), shifted from 1655 cm⁻¹ (uncomplexed (*R,R*)-BOX (Ph) on a resin) (Scheme 6D vs. 6B and 6C). We did not observe any thermal stability differences on the resin between (*SS,RR*)-Zn(II) BOX (Ph/Ph) and (*SS,RR*)-Zn(II) BOX (Me/Ph) through a temperature range tested (up to 160 °C in *d*₆-DMSO). In addition, no ligand exchange took place when additional (*S,S*)-BOX (Ph) or (*S,S*)-BOX (Me) was further mixed with the above dual-function-

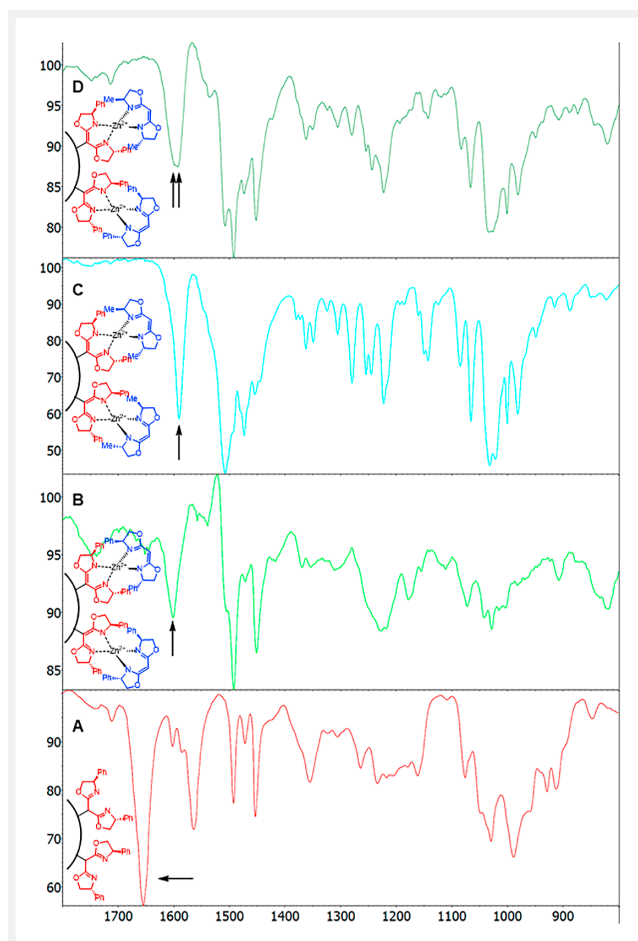


Figure 5 FTIR comparison of A) (*R,R*)-BOX (Ph)-functionalized Wang resin, B) (*RR,SS*)-BOX (Ph/Ph)-functionalized Wang resin, C) (*RR,SS*)-BOX (Ph/Me)-functionalized Wang resin, D) (*RR,SS*)-BOX (Ph/Ph)- and (*RR,SS*)-BOX (Ph/Me)-functionalized Wang resin.

alized resin. For example, when 10 equiv of (*S,S*)-BOX (Me) was mixed with (*SS,RR*)-Zn(II) BOX (Ph/Ph)/(*SS,RR*)-Zn(II) BOX (Me/Ph) dual-functionalized resin, no (*S,S*)-BOX (Ph) was released into the supernatant solution after 72 h at ambient temperature. In addition, both FTIR C=N stretch signals (1598 cm⁻¹ and 1593 cm⁻¹) remained the same after the resulting resins were washed several times.

These observations have led us to believe the alteration of the ratio of loading functional group can be possible by simply adjusting the mixture ratio of chiral BOX ligands. Indeed, when a ligand mixture consisting of 1:3 ratio of (*S,S*)-BOX (Me) and Fmoc-functionalized (*S,S*)-BOX (Ph) was mixed with (*R,R*)-BOX (Ph)-immobilized resin in the presence of Zn(OAc)₂, the ratio of bound ligands (>98% saturation on loading capacity) was identical (1:3) to the added free ligand mixture (entry 3). An identical result was obtained when the same mixture was used in excess molar amount (entry 4). These results indicate that the ratio of loaded

Table 4 A dual functionalization of Wang resin

Entry	Added ligands ^{a,b}	Product ^c	
		Bound	Unbound
1	(<i>S,S</i>)-BOX (Ph) (0.5 equiv)	>98%	ND ^e
	(<i>S,S</i>)-BOX (Me) (0.5 equiv)		
2	(<i>R,R</i>)-BOX (Ph) (0.5 equiv)	32%	68%
	(<i>R,R</i>)-BOX (Me) (0.5 equiv)		
3	(<i>S,S</i>)-BOX (Ph) (0.25 equiv)	>98%	ND ^e
	(<i>S,S</i>)-BOX (Me) (0.75 equiv)		
4	(<i>S,S</i>)-BOX (Ph) (1.0 equiv)	25%	75%
	(<i>S,S</i>)-BOX (Me) (3.0 equiv)	(>98%) ^d	

^a 1 equiv of free ligand = 0.28 mmol per 1.0 g of BOX-functionalized resin; ^b Equimolar amount of Zn(OAc)₂ was used in all cases. ^c Bound/unbound ligands are calculated based on 1) quantification of bound ligands upon their detachment from resin through EDTA treatment, and 2) quantification of unbound complexes in the supernatant solution; ^d Based on resin loading capacity. ^e ND: not detected.

functional groups can be precisely controlled by altering the mixture ratio of added functional groups.

Conclusions

In summary, the chirality-directed self-assembly of heteroleptic Zn(II) complexes can be used as a strategy to load multiple functional groups on resin. Due to the high selectivity toward forming heteroleptic Zn(II) complexes, this straightforward process can be used without purification because there are no by-products formed. The selectivity toward the formation of heterochiral Zn(II) core complexes was not influenced by the size of the chiral substituents on the BOX ligand. The resin-generated heteroleptic Zn(II) complexes are stable at elevated temperatures; however, they can be easily disassembled through treatment by EDTA for resin recyclization. In theory, this methodology enables to functionalize a range of solid supports such as graphene, metal nanoparticles, and various polymer-based materials. Further studies are currently in progress, including theoretical calculations of various homo- and heterochiral BOX Zn(II) complexes.

Experimental Section

General Information: Solvents and materials were obtained from commercial suppliers (Fisher Scientific, Sigma-Aldrich, and Alfa Aesar) and used without further purification. Unless otherwise noted, all reactions were performed in standard dry glassware under an Argon atmosphere in dry solvents. Evaporation and concentration of solvents were carried out with Büchi Rotavapor R-200 attached to a Maxima-dry vacuum pump. Roto-evaporation for all zinc complexes was performed at ambient temperature, and the residue was further dried under a high vacuum to obtain the complexed products. THF used for the synthesis of substituted box derivatives was dried using 4 Å molecular sieves. Preparative separations were performed by silica gel gravity column chromatography using Silica Flash P60. TLC analyses were performed on Merck Kieselgel 60 F254 glass plates and were visualized with UV light or stains (iodine, vanillin, ninhydrin). ¹H NMR and ¹³C NMR spectra were recorded at 25 °C on a Varian 400 MHz spectrometer using CDCl₃ and DMSO-*d*₆ as solvents, which were purchased from Sigma Aldrich and Cambridge Isotope Laboratories, respectively. The solvent signals were used as internal standards for both ¹H NMR (CDCl₃ δ = 7.26 ppm) and ¹³C NMR (CDCl₃ δ = 77.20 ppm) recordings. ¹H NMR data are reported as follows: chemical shift (reported in parts per million), multiplicity (s = singlet, d = doublet, t = triplet, quart = quartet, quint = quintet, sext = sextet, sept = septet, br = broad, and m = multiplet), integration, and coupling constants (reported in hertz). Mass spectra were measured with a Thermo Fisher Scientific Q Exactive Plus (ESI, APCI) spectrometer and an ABI 4700 mass spectrometer. Infrared spectra were collected on a Nicolet iS10 FTIR spectrometer using a Smart iTR-attenuated total reflectance sampling accessory with a single bounce ZnSe crystal plate. Polarimetry was measured in a Perkin Elmer Model 341 polarimeter at 25 °C in a 100 mm cell at 589 nm using CH₂Cl₂ as the solvent.

General Procedure for Preparation of Chiral BOX Ligands: (*R,R*)- or (*S,S*)-BOX ligands were prepared according to the published procedure.²⁴

(*R,R*)- or (*S,S*)-BOX (Ph): To a solution of diethyl malonimide dihydrochloride (90 mmol) in dichloromethane (600 mL) was added the amino alcohol (98 mmol, 2.2 equiv) at room temperature. The reaction mixture was stirred under reflux for 48 h, and water (150 mL) was added to the reaction mixture. The crude product was extracted using dichloromethane (3 × 100 mL), and the combined organic layers were washed with brine (2 × 200 mL). Solvents were evaporated under reduced pressure, and the crude product was purified by column chromatography with DCM/MeOH (19:1) as the eluent to give pure chiral BOX ligands. (*S,S*)-BOX (Ph): pale brown oil; ¹H NMR (400 MHz, CDCl₃): δ 7.35–7.17 (m, 10 H), 5.25 (dd, *J* = 9.8, 8.3 Hz, 2 H), 4.67 (dd, *J* = 10.2, 8.4 Hz, 2 H), 4.17 (dd, *J* = 8.4, 7.9 Hz, 2 H), 3.57 (s, 2 H)

ppm. ^{13}C NMR (101 MHz, CDCl_3): δ 163.00, 142.03, 128.69, 127.58, 126.64, 75.31, 69.74, 28.39 ppm. MS (ESI): m/z calculated for $\text{C}_{19}\text{H}_{18}\text{N}_2\text{O}_2$ $[\text{M} + \text{H}]^+$, 307.1441; found, 307.1427.

General Procedure for Preparation of Homochiral Zn(II) BOX Complexes: (*SS,SS*)-Zn(II) BOX (Ph) was prepared according to the published procedure.²⁴ To a solution of (*S,S*)-BOX (Ph) (2.0 g, 6.53 mmol) in dichloromethane (10 mL) was added $\text{Zn}(\text{OAc})_2$ (600 mg, 3.26 mmol) in methanol (5 mL) and the resulting reaction mixture was stirred for 1 min and solvents are removed under reduced pressure to give 2.1 g (> 95%) of pure (*SS,SS*)-Zn(II) BOX (Ph) as a clear crystal. ^1H NMR (400 MHz, CDCl_3) δ 7.20–7.10 (m, 12 H), 6.88 (dd, $J = 6.2, 3.0$ Hz, 8 H), 4.54 (t, $J = 8.5$ Hz, 4 H), 4.32 (t, $J = 8.4$ Hz, 4 H), 3.95 (s, 2 H), 3.77 (t, $J = 8.4$ Hz, 4 H) ppm. ^{13}C NMR (101 MHz, CDCl_3) δ 171.92, 141.03, 128.47, 127.64, 126.72, 73.34, 66.52, 54.30 ppm. MS (ESI): m/z calculated for $\text{C}_{38}\text{H}_{35}\text{N}_4\text{O}_4\text{Zn}$ $[\text{M} + \text{H}]^+$, 675.1993; found, 675.1802.

General Procedure for Preparation of Heterochiral Zn(II) BOX Complexes: (*SS,RR*)-Zn(II) BOX (Ph) was prepared according to the published procedure.²⁴ To a solution of (*S,S*)-BOX (Ph) (1.0 g, 3.26 mmol) in dichloromethane (5 mL) was added (*R,R*)-BOX (Ph) (1.0 g, 3.26 mmol) in dichloromethane (5 mL) at room temperature. $\text{Zn}(\text{OAc})_2$ (600 mg, 3.26 mmol) in methanol (5 mL) was added to the mixture, and the resulting reaction mixture was stirred for 1 min, and the solvents were removed under reduced pressure to give pure (*SS,RR*)-Zn(II) BOX (Ph) as white crystals. ^1H NMR (400 MHz, CDCl_3): δ 7.34–7.26 (m, 8 H), 7.25–7.18 (m, 4 H), 7.12–6.99 (m, 8 H), 4.05 (dd, $J = 8.3, 5.2$ Hz, 4 H), 3.89 (t, $J = 8.7$ Hz, 4 H), 3.38 (dd, $J = 9.1, 5.2$ Hz, 4 H) ppm.

General Procedure for Generation of Two Specific Sets of Heterochiral Zn(II) Complexes: Mixtures of (*SS,RR*)-Zn(II) BOX (Me/Ph) and (*SS,RR*)-Zn(II) BOX (Me/Ph) were prepared in one pot by simply mixing (*RR,RR*)-Zn(II) BOX (Ph/Ph), (*SS,SS*)-Zn(II) BOX (Me/Me) and (*SS,SS*)-Zn(II) BOX (Ph/Ph) in a 2:1:1 ratio. The mixture was a white powder. ^1H NMR (600 MHz, CDCl_3): δ 7.33–7.17 (m, 24 H), 7.10–7.03 (m, 8 H), 4.83 (dd, $J = 8.9, 5.6$ Hz, 2 H), 4.50 (t, $J = 8.8$ Hz, 2 H), 4.31 (dd, $J = 8.6, 5.6$ Hz, 2 H), 4.15 (s, 1 H), 4.06 (dd, $J = 8.2, 5.3$ Hz, 4 H), 3.89 (t, $J = 8.7$ Hz, 4 H), 3.87 (s, 2 H), 3.78 (t, $J = 8.1$ Hz, 2 H), 3.64 (s, 1 H), 3.45 (t, $J = 7.4$ Hz, 2 H), 3.38 (dd, $J = 9.1, 5.2$ Hz, 4 H), 2.69 (m, $J = 6.7$ Hz, 2 H), 0.97 (d, $J = 6.3$ Hz, 6 H) ppm.

Generation of Dual-Heterochiral Zn(II) Complexes on the Wang Resin: The (*R,R*)-BOX-functionalized resin (*R,R*)-SI-2 (3.00 g, 0.278 mmol/g) was suspended in dry DCM and stirred at ambient temperature for 1 h. To the solution was added (*S,S*)-BOX (Ph) (128 mg, 0.42 mmol) and (*S,S*)-BOX (Me) (76 mg, 0.42 mmol) in DCM (2 mL), and the mixture was stirred for 1 min. A solution of $\text{Zn}(\text{OAc})_2$ (153 mg, 0.84 mmol) in MeOH (2.0 mL) was added to the mixture and stirred for 10 min at room temperature. The resin was removed by filtration and washed with DCM (3×10 mL), followed by diethyl ether (3×10 mL). FTIR: 1598 cm^{-1} ((*SS,RR*)-

Zn(II) BOX (Ph/Ph)) and 1593 cm^{-1} ((*SS,RR*)-Zn(II) BOX (Me/Ph)).

Funding Information

This work is supported by the National Science Foundation under grant number 1856522.

Supporting Information

Supporting Information for this article is available online at <https://doi.org/10.1055/a-2106-9071>.

Conflict of Interest

The authors declare no conflict of interest.

References

- (1) Miceli, M.; Frontera, P.; Macario, A.; Malara, A. *Catalysts* **2021**, *11*, 591.
- (2) Whitesides, G. M.; Grzybowski, B. *Science* **2002**, *295*, 2418.
- (3) (a) Xiao, W.; Li, B.; Yan, J.; Wang, L.; Huang, X.; Gao, J. *Composites, Part A* **2023**, *165*, 107335. (b) Li, Z.; Fan, Q.; Yin, Y. *Chem. Rev.* **2022**, *122*, 4976. (c) Sinha, N. J.; Langenstein, M. G.; Pochan, D. J.; Kloxin, C. J.; Saven, J. G. *Chem. Rev.* **2021**, *121*, 13915. (d) Chen, S.; Costil, R.; Leung, F. K.-C.; Feringa, B. L. *Angew. Chem. Int. Ed.* **2021**, *60*, 11604.
- (4) (a) Heiner, B. R.; Pittsford, A. M.; Kandel, S. A. *Chem. Commun.* **2023**, *59*, 170. (b) Mayerhoefer, E.; Krueger, A. *Acc. Chem. Res.* **2022**, *55*, 3594. (c) Li, K.; Yang, J.; Gu, J. *Acc. Chem. Res.* **2022**, *55*, 2235.
- (5) Susam, Z.D.; Tanyeli, C. *Asian J. Org. Chem.* **2021**, *10*, 1251.
- (6) Komaromy, D.; Stuart, M. C. A.; Monreal Santiago, G.; Tezcan, Meniz; Krasnikov, V. V.; Otto, S. N. *J. Am. Chem. Soc.* **2017**, *139*, 6234.
- (7) (a) Lombardo, M.; Trombini, C. *Green Chem.* **2009**, *3*, 1. (b) Barbaro, P.; Liguori, F. *Chem. Rev.* **2009**, *109*, 515. (c) Heitbaum, M.; Glorius, F.; Escher, I. *Angew. Chem. Int. Ed.* **2006**, *45*, 4732. (d) Horn, J.; Michalek, F.; Tzschucke, C. C.; Bannwarth, W. *Top. Curr. Chem.* **2004**, *242*, 43.
- (8) (a) Wang, T.; Menard-Moyon, C.; Bianco, A. *Chem. Soc. Rev.* **2022**, *51*, 3535. (b) Lou, J.; Sagar, R.; Best, M. D. *Acc. Chem. Res.* **2022**, *55*, 2882. (c) Liu, Z.; Zhou, Y.; Yuan, L. *Org. Biomol. Chem.* **2022**, *20*, 9023.
- (9) Boott, C. E.; Nazemi, A.; Manners, I. *Angew. Chem. Intl. Ed.* **2015**, *54*, 13876.
- (10) Gruttadauria, M.; Giacalone, F.; Noto, R. *Green Chem.* **2013**, *15*, 2608.
- (11) Menuet, E.M.; Zhou, J.; Tian, S.; Brenner, R. E.; Ren, Z.; Hua, D. H.; Kilway, K. V.; Moteki, S. A. *Org. Biomol. Chem.* **2022**, *20*, 4314.
- (12) (a) Takacs, J. M.; Moteki, S. A.; Reddy, D. S. *Supramolecular Catalysis*. van Leeuwen, P. W. N. M. Wiley-VCH: Weinheim, **2008**; 235. (b) Atkins, J. M.; Moteki, S. A.; DiMagno, S. G.; Takacs, J. M. *Org. Lett.* **2006**, *8*, 2759.

- (13) (a) Thacker, N. C.; Moteki, S. A.; Takacs, J. M. *ACS Catal.* **2012**, *2*, 2743. (b) Moteki, S. A.; Toyama, K.; Liu, Z.; Ma, J.; Holmes, A. E.; Takacs, J. M. *Chem. Commun.* **2012**, *48*, 263. (c) Moteki, S. A.; Takacs, J. M. *Angew. Chem. Int. Ed.* **2008**, *47*, 894.
- (14) Takacs, J. M.; Hrvatin, P. M.; Atkins, J. M.; Reddy, D. S.; Clark, J. L. *New J. Chem.* **2005**, *29*, 263.
- (15) Zhou, J.; Cole, A. M.; Menuey, E. M.; Kilway, K. V.; Moteki, S. A. *Chem. Commun.* **2021**, *57*, 6404.
- (16) (a) Liu, M.; Wu, J.; Hou, H. *Chem. Eur. J.* **2019**, *25*, 2935. (b) Ye, R.; Zhukhovitskiy, A. V.; Deraedt, C. V.; Toste, F. D.; Somorjai, G. A. *Acc. Chem. Res.* **2017**, *50*, 1894.
- (17) The ratio between heterochiral and homochiral Zn(II) complexes was 68: 32 (in d2-TCE) at 50 °C in favor of the heterochiral Zn(II) complex.
- (18) See the Supporting Information for full ¹H NMR comparisons.
- (19) See the Supporting Information for spectroscopic details.
- (20) Carreiro, E. P.; Moura, N. M. M.; Burke, A. J.; Anthony, J. *Eur. J. Org. Chem.* **2012**, *3*, 518.
- (21) Buszek, K. R.; Brown, N. *J. Org. Chem.* **2007**, *72*, 3125.
- (22) (a) Carneiro, L.; Silva, A. R.; Shuttleworth, P. S.; Budarin, V.; Clark, J. H. *Molecules* **2014**, *19*, 11988. (b) Silva, A. R.; Guimaraes, V.; Carvalho, A. P.; Pires, J. *Catal. Sci. Technol.* **2013**, *3*, 659.
- (23) We were unable to differentiate between homochiral Zn(II) complexes and heterochiral Zn(II) complexes using FTIR.
- (24) Takacs, J. M.; Reddy, D. S.; Moteki, S. A.; Wu, D.; Palencia, H. *J. Am. Chem. Soc.* **2004**, *126*, 4494.